analytical chemistry

Letter

Cite This: *Anal. Chem.* 2019, 91, 11510−11513

pubs.acs.org/ac

Naked-Eye Detection of Grapevine Red-Blotch Viral Infection Using a Plasmonic CRISPR Cas12a Assay

Yongya Li,[†,‡] Hayam Mansour,[‡,§] Tony Wang,[∥] Sudarsana Poojari,[∥] and Feng Li*[,†,‡]

[†]College of Chemistry, Sichuan University, Chengdu, Sichuan 610064, P.R. China

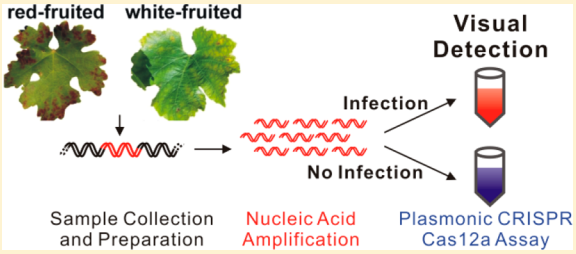
[‡]Department of Chemistry, Centre for Biotechnology, Brock University, St. Catharines, Ontario L2S 3A1, Canada

[§]Department of Cell Biology, National Research Centre, Cairo 12622, Egypt

[∥]Cool Climate Oenology and Viticulture Institute, Brock University, St. Catharines, Ontario L2S 3A1, Canada

Supporting Information

ABSTRACT: Herein, we described a novel plasmonic CRISPR Cas12a assay for the visual, colorimetric detection of grapevine viral infections. Our assay generates rapid and specific colorimetric signals for nucleic acid amplicons by combining the unique target-induced incriminate single-stranded DNase activity of Cas12a with plasmon coupling of DNA functionalized gold nanoparticles. The practical applicability of our plasmonic assay was successfully demonstrated through the detection of emerging red-blotch viral infections in grapevine samples collected from commercial vineyards.



Downloaded via 23.238.128.118 on November 7, 2020 at 08:09:33 (UTC).
See https://pubs.acs.org/sharingguidelines for options on how to legitimately share published articles.

The grape and wine industry has an estimated annual impact of over $300 billion U.S. dollars (USD) worldwide. However, the profitable and sustainable grape production is currently threatened by diseases caused by viral and other pathogenic infections.[1] The emerging grapevine red-blotch virus (GRBV) infection alone is estimated to cause economical loses in the range of $2 231 to $68 548 (USD) per hectare per year.[2,3] The effective treatment and management of grapevine viral infections require diagnostic tests capable of rapid detection and routine monitoring of disease outbreaks in infrastructure-constrained settings such as vineyard and nurseries.[1−9] Toward this need, we aim to develop a visual, colorimetric molecular diagnostic test for the rapid and accurate detection of grapevine viral infections.

GRBV is a single-stranded circular DNA virus that infects grapevines of all varieties and is internationally present.[2−4] Although GRBV infected red-berried cultivars of *Vitis Vinefera L.* can show characteristic symptoms on the mature leaves at postveraison but such symptoms are less apparent on white-berried cultivars and interspecific hybrids (Figure 1A and Figure S1). Symptoms of GRBV can also be confused with other viruses, such as the grapevine leafroll-associated viruses that infect grapevines. As such, rapid and in-field detection of GRBV at the genetic level is critical to allow accurate diagnosis for timely management. However, standard nucleic acid tests (NATs) for GRBV are performed predominately at centralized laboratories using polymerase chain reaction (PCR) followed by gel electrophoresis analyses.[5] Other NATs, such as quantitative PCR (qPCR) and digital PCR (dPCR), have recently been deployed for GRBV diagnosis but rely on expensive and bulky instrument for signal readout.[6−8] Miniaturization of standard NAT for grapevine viral infections requires not only portable thermal cyclers or isothermal PCR-alternatives but also visual, colorimetric readouts to facilitate the rapid signal generation and decision making.[9] Herein, we introduce a novel plasmonic CRISRP Cas12a assay via the integration of target-induced CRISPR single-stranded DNase (ssDNase) activation and color transition mediated by plasmonic gold nanoparticles (AuNPs). By combining the plasmonic CRISPR Cas12a assay with PCR, we demonstrate the visual, colorimetric detection of GRBV infections in diverse grapevine samples collected from commercial vineyards.

Recent advances in CRISPR (Clustered Regularly Interspaced Short Palindromic Repeats) and CRISPR associated (Cas) enzymes have revealed unique collateral DNase activities of Cas12a.[10,11] By equipping CRISPR Cas12a with recombinase polymerase amplification (RPA) and fluorogenic substrates, Doudna and co-workers have invented a DNA endonuclease-targeted CRISPR trans reporter (DETECTR) for rapid and specific detection of human papillomavirus in patient samples.[11] Our plasmonic CRISPR Cas12a assay is inspired by DETECTR but using DNA functionalized AuNPs to generate sensitive visual readout for PCR amplicons. Plasmonic nanoparticles, such as AuNPs, are highly efficient colorimetric readout that has been widely deployed for the sensitive detection of nucleic acids and proteins.[12−18] Figure 1A shows a typical workflow of our assay for analyzing genetic viral markers in a grapevine sample. Total nucleic acids are first extracted and amplified using standard extraction, PCR protocols, and virus specific primers. The sequence-specific recognition is achieved through a CRISPR RNA (crRNA) that

Received: August 4, 2019
Accepted: September 3, 2019
Published: September 3, 2019

ACS Publications © 2019 American Chemical Society

DOI: 10.1021/acs.analchem.9b03545
Anal. Chem. 2019, 91, 11510−11513

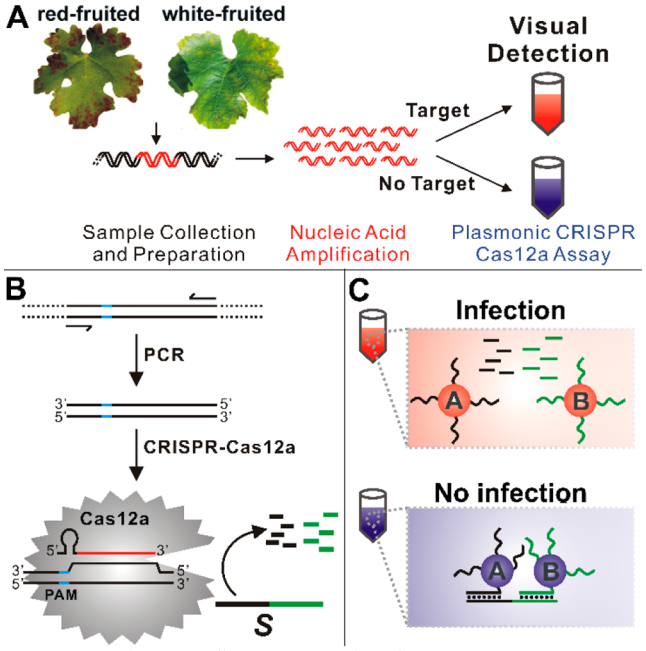


Figure 1. Schematic illustration of the plasmonic CRISPR Cas12a assay for the detection of grapevine viral infection. (A) Workflow for visual detection of GRBV infections in red-fruited and white-fruited grapevine samples. (B) Target recognition using CRISPR-Cas12a and the activation of incriminate ssDNase activity. (C) Color development using plasmonic DNA functionalized AuNPs.

also recruits a Cas12a protein and unleashes its indiscriminative ssDNase activity (Figure 1B). As a result, a single-stranded substrate (S) will be completely degraded in the presence of the genetic viral marker and subsequent PCR amplicon. S also serves as a linker that cross-links two DNA functionalized AuNPs, AuNP-A and AuNP-B, through hybridization (Figure 1C). It has been well-established that upon cross-linking, the close proximity of AuNPs leads to coupling of their individual localized plasmon fields and thus a red-to-blue color transition.[12−16] However, in the presence of the viral marker, S is degraded by Cas12a and the AuNP solution thus remains to be red. Therefore, by simply examining the color of the assay solution using the naked-eye, we will be able to determine the presence (red) or absence (blue) of the viral infection. Moreover, as the sequence of S is independent of that of the target, the same plasmonic readout system can be generalized to any target of interest without any modification.

We first set out to examine the AuNP-based plasmonic readout. The concentration of the linker S is a critical parameter for resulting in a visual color change of the AuNP solution. In our experiments, we fixed the concentration of AuNP-A and AuNP-B to be 500 pM and varied the concentration of S from 0 to 50 nM. As shown in Figure 2A, the red-to-blue color transition occurs at 10 nM and saturated at 30 nM. We also measured the absorbance spectrum for each sample for quantitative monitoring of the color change (Figure 2B). Consistent with the visual observation, the maximum absorbance λ_{max} shifted from 526 to 560 nm when varying the S concentration from 0 to 50 nM (Figure 2C). As 30 nM is the minimal concentration resulting in a complete color transition, this concentration was used as an optimal parameter for the subsequent assay development.

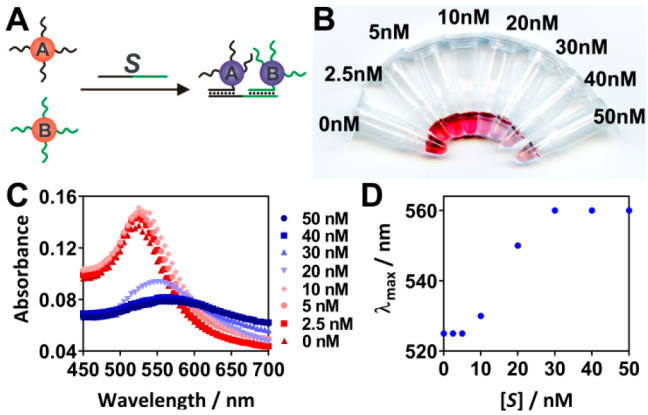


Figure 2. (A) Schematic illustration of the plamonic readout using DNA-AuNPs. (B) Color transitions of AuNPs in the presence of varying concentrations of the linker S. (C) Absorbance spectra of DNA-AuNPs in the presence of S. (D) Maximum absorbance λ_{max} as a function of varying concentrations of S.

We next examined the compatibility of the plasmonic readout to the CRISPR Cas12a system. A 35-bp dsDNA containing a 5′ TTTA protospacer-adjacent motif (PAM) was used as a model target. A crRNA was designed to contain 20-nt target-dependent sequence and a RNA scaffold to assist the detection of dsDNA target in a PAM-dependent manner. We found that crRNA and Cas12a interfered with S for cross-linking AuNP-A and AuNP-B even in the absence of the target, which results in very little color change and shift of λ_{max} (Figure S2A). An extended incubation time from 5 to 15 min was found to restore the color change and promote the shift of λ_{max} by 8 times (Figure S2B). By analyzing target dsDNA from 0.1 pM to 1 nM using the plasmonic CRISPR Cas12a assay with the S concentration fixed at 30 nM, we found a sharp color transition at 200 pM (Figure 3A), with a detection limit of 40 pM determined using the spectra shifts (Figure 3B). It is also possible to fine-tune the dynamic range of our assay by simply altering the concentration of S. As shown in Figure 3B,

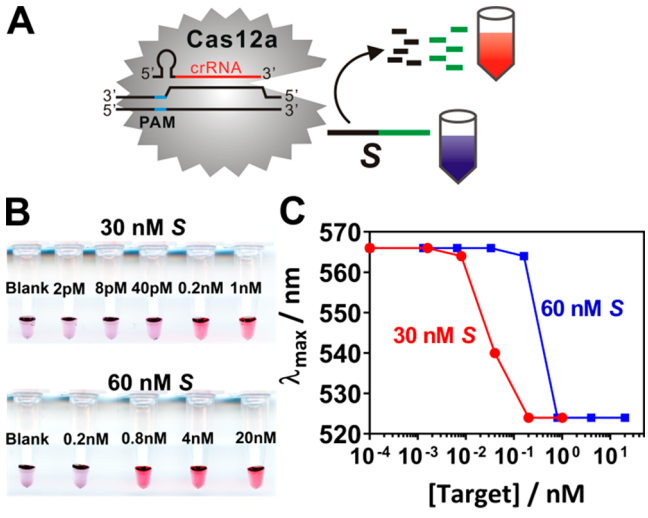


Figure 3. (A) Schematic illustration of the plasmonic CRISPR Cas12a assay. (B) Images for visual detection of target dsDNA using plasmonic CRISPR Cas12a assays with 30 nM or 60 nM S. (C) Maximum absorbance λ_{max} as a function of varying target concentrations.

DOI: 10.1021/acs.analchem.9b03545
Anal. Chem. 2019, 91, 11510−11513

by using 60 nM S, the sharp color transition was found shifted to 800 pM.

Having verified that the plasmonic readout is fully compatible with CRISPR Cas12a, we next challenged our plasmonic assay for diagnosing GRBV infections in grapevine samples. We first verified our assay for the detection of PCR amplicons generated from a 130-bp synthetic DNA standard corresponding to a subgenome of GRBV at a location from 2 753 to 2 882 of the reference genome (JQ901105).[19] To enable CRISPR Cas12a recognition, a crRNA was designed to target a 20-nt sequence right after a 5′-TTTG PAM domain. We found that our plasmonic assay is fully compatible with PCR, and clear red solutions were observed for targets with concentrations varying from 10 aM to 1 pM (Figure S3). A blue color was observed in the absence of the target (blank). Having observed this exciting result, we next challenged our assay using real GRBV samples collected from infected grapevine leaves (Figure 4B). As a comparison, we also

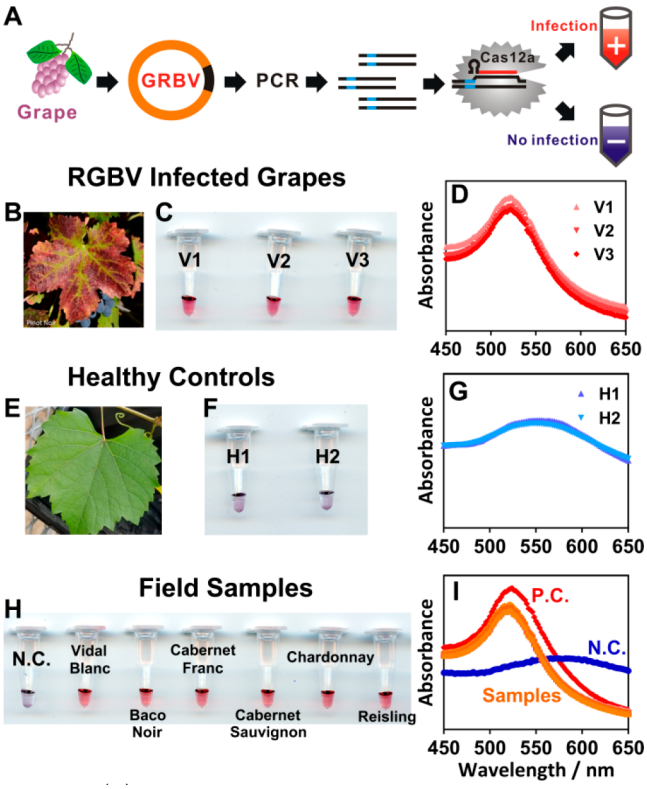


Figure 4. (A) Schematic illustration of the visual detection of GRBV infection in grape samples using PCR and plasmonic CRISPR Cas12a assay, (B) image of a representative leaf of a GRBV infected grape, (C) images for visual detection of GRBV infection for GRBV positive plants, (D) absorbance spectra of GRBV positive tests, (E) image of a representative leaf of a healthy grape, (F) images for visual tests of healthy controls, (G) absorbance spectra of GRBV negative tests in healthy controls, (H) images for visual detection of GRBV infection for field samples collected in 2018, and (I) absorbance spectra of GRBV tests for field samples.

extracted total DNA from leaves of healthy controls (Figure 4E). As shown in Figure 4C, all three infected samples produce red colors upon PCR amplification and color development. By contrast, the two healthy controls produce blue colors, which were the same as the blank (Figure 4F). All results were consistent with the standard polyacrylamide gel electrophoresis (PAGE) analyses (Figure S4). These results suggest that our assay is suitable for visual diagnosis of grapevine viral infections and holds the potential for field-based uses.

We finally challenged our assay for analyzing real grapevine samples collected in the field. Six grapevine samples representing both white- (Vidal blanc) and red-fruited (Baco Noir) interspecific hybrids as well as white- (Chardonnay and Riesling) and red-fruited (Cabernet Franc and Cabernet Sauvignon) *V. vinifera* cvs were collected from commercial vineyard blocks in Niagara, Canada. Total nucleic acids were extracted from petiole samples. All six samples were found to be GRBV infected using our plasmonic assay, evidenced by the red-colored reaction solutions (Figure 4H). This result was further confirmed using standard end-point polymerase chain reaction (PCR) followed by analyses using agarose gel electrophoresis (Figure S5) and droplet digital PCR (Figure S6). To test the robustness of assay for field applications, we also made a dilution series for each sample. As shown in Figure S7, we found that accurate diagnostic results could be obtained for samples subject to 2 000−10 000 dilutions, suggesting that our assay is highly robust and can tolerate substantial DNA loss often occurring during sample pretreatment in the field.

In conclusion, we have developed a novel plasmonic CRIPSR Cas12a assay that generates a visual, colorimetric readout for nucleic acid tests deployable to the fields. Our assay can act as a simple "add-on" color developer to the existing PCR or isothermal nucleic acid amplification protocols and readily converts them into visual colorimetric tests. We successfully demonstrated the practical applicability of our assay for the rapid detection of viral infections in grapevine samples. Because of the effectiveness and simplicity, we anticipate that our plasmonic CRISPR Cas12a assay will find broad applications to nucleic acid testing in the diagnosis and management of both human and crop infections.

■ ASSOCIATED CONTENT

Supporting Information

The Supporting Information is available free of charge on the ACS Publications website at DOI: 10.1021/acs.analchem.9b03545.

Experimental details; DNA sequence and modifications; and additional data and spectra (PDF)

■ AUTHOR INFORMATION

Corresponding Author

*E-mail: fli@brocku.ca.

ORCID

Feng Li: 0000-0002-2616-5343

Notes

The authors declare no competing financial interest.

■ ACKNOWLEDGMENTS

We thank the Fundamental Research Funds for the Central Universities, the National Sciences and Engineering Research Council of Canada, and the Ontario Ministry of Research, Innovation and Science for the financial support.

■ REFERENCES

(1) Xiao, H.; Shabanian, M.; Moore, C.; Li, C.; Meng, B. *Virol. J.* **2018**, *15*, 127.

DOI: 10.1021/acs.analchem.9b03545
Anal. Chem. 2019, 91, 11510−11513

(2) Ricketts, K. D.; Gomez, M. I.; Fuchs, M. F.; Martinson, T. E.; Smith, R. J.; Cooper, M. L.; Moyer, M. M.; Wise, A. *Am. J. Enol. Vitic.* **2017**, *68*, 127−135.
(3) Cieniewicz, E. J.; Pethybridge, S. J.; Loeb, G.; Perry, K.; Fuchs, M. *Phytopathology* **2018**, *108*, 94−102.
(4) Girardello, R. C.; Cooper, M. L.; Smith, R. J.; Lerno, L. A.; Bruce, R. C.; Eridon, S.; Oberholster, A. *J. Agric. Food Chem.* **2019**, *67*, 5496−5511.
(5) Sudarshana, M. R.; Perry, K. L.; Fuchs, M. F. *Phytopathology* **2015**, *105*, 1026−1032.
(6) Setiono, F. J.; Chatterjee, D.; Fuchs, M.; Perry, K. L.; Thompson, J. R. *Plant Dis.* **2018**, *102*, 2187−2193.
(7) Poojari, S.; Alabi, O. J.; Okubara, P. A.; Naidu, R. A. *J. Virol. Methods* **2016**, *235*, 112−118.
(8) Bahder, B. W.; Zalom, F. G.; Jayanth, M.; Sudarshana, M. R. *Phytopathology* **2016**, *106*, 1223−1230.
(9) Romero Romero, J. L.; Carver, G. D.; Arce Johnson, P.; Perry, K. L.; Thompson, J. R. *Arch. Virol.* **2019**, *164*, 1453−1457.
(10) Zetsche, B.; Gootenberg, J. S.; Abudayyeh, O. O.; Slaymaker, I. M.; Makarova, K. S.; Essletzbichler, P.; Volz, S. E.; Joung, J.; van der Oost, J.; Regev, A.; Koonin, E.; Zhang, F. *Cell* **2015**, *163*, 759−771.
(11) Chen, J. S.; Ma, E.; Harrington, L. B.; Da Costa, M.; Tian, X.; Palefsky, J. M.; Doudna, J. A. *Science* **2018**, *360*, 436−440.
(12) Elghanian, R.; Storhoff, J. J.; Mucic, R. C.; Letsinger, R. L.; Mirkin, C. A. *Science* **1997**, *277*, 1078−1081.
(13) Zagorovsky, K.; Chan, W. C. W. *Angew. Chem.* **2013**, *125*, 3250−3254.
(14) Valentini, P.; Pompa, P. P. *Angew. Chem., Int. Ed.* **2016**, *55*, 2157−2161.
(15) Smith, B. D.; Dave, N.; Huang, P.-J. J.; Liu, J. *J. Phys. Chem. C* **2011**, *115*, 7851−7857.
(16) Song, T.; Xiao, S.; Yao, D.; Huang, F.; Hu, M.; Liang, H. *Adv. Mater.* **2014**, *26*, 6181−6185.
(17) de la Rica, R.; Stevens, M. M. *Nat. Nanotechnol.* **2012**, *7*, 821−824.
(18) Liu, D.; Wang, Z.; Jin, A.; Huang, X.; Sun, X.; Wang, F.; Yan, Q.; Ge, S.; Xia, N.; Niu, G.; Liu, G.; Hight Walker, A. R.; Chen, X. *Angew. Chem., Int. Ed.* **2013**, *52*, 14065−14069.
(19) Krenz, B.; Thompson, J. R.; McLane, H. L.; Fuchs, M.; Perry, K. L. *Phytopathology* **2014**, *104*, 1232−1240.

DOI: 10.1021/acs.analchem.9b03545
Anal. Chem. 2019, 91, 11510−11513